This is a repository copy of *Inorganically modified clay minerals: Preparation, characterization, and arsenic adsorption in contaminated water and soil*.

White Rose Research Online URL for this paper:
http://eprints.whiterose.ac.uk/126765/

Version: Accepted Version

Article:

1 **Inorganically modified clay minerals: preparation, characterization, and arsenic adsorption**

2 **in contaminated water and soil**

3

4 Raj Mukhopadhyay[a], K. M. Manjaiah[a*], S. C. Datta[a], R. K. Yadav[b], Binoy Sarkar[c,d]

5

6 [a]Division of Soil Science and Agricultural Chemistry, ICAR-Indian Agricultural Research

7 Institute, New Delhi 110012, India

8 [b]Division of Soil and Crop Management, ICAR-Central Soil Salinity Research Institute, Karnal,

9 Haryana 132001, India

10 [c] Department of Animal and Plant Sciences, The University of Sheffield, Sheffield, S10 2TN, UK

11 [d]Future Industries Institute, University of South Australia, Mawson Lakes, SA 5095, Australia

12

13 *Correspondence to: K. M. Manjaiah, Division of Soil Science and Agricultural Chemistry, ICAR-

14 Indian Agricultural Research Institute, New Delhi 110012, India.

15 E-mail address: manjaiah@iari.res.in (K. M. Manjaiah).

16

17 **Abstract**

18 The use of modified clay minerals for adsorbing arsenic (As) in contaminated soils is an

19 underexplored area of research. The adsorption behavior of As onto inorganically modified

20 smectite and kaolinite both in aqueous and soil media was studied. X-ray diffraction, infra-red

21 spectroscopy, scanning and transmission electron microscopy studies confirmed successful

22 modification of smectite through Fe-exchange and Ti-pillaring, and kaolinite through phosphate

23 binding. The modified smectites were more efficient than phosphate-bound kaolinite in adsorbing

As both in water and soil systems. Kinetic study revealed that the clay products reached adsorption equilibrium within 3 h, and the data well fitted to the power function and simple Elovich equation ($R^2 > 0.90$). The Freundlich isotherm model best described the As adsorption data ($R^2 > 0.86$) of the modified clay products in both the systems. The Ti-pillared smectite exhibited the highest As adsorption capacity (156.54 $\mu g g^{-1}$) in the aqueous medium, while the Fe-exchanged smectite was the best material in the soil system (115.63 $\mu g g^{-1}$). The partition coefficient (K_d) and adsorption efficiency (%) data also maintained the similar trend. Precipitation of As and binuclear complex formation also took place in the soil system which made the metalloid non-labile as the time passed. The inorganically modified clay products reported here hold a great potential to adsorb As in contaminated groundwater, drinking water as well as soil.

Key words: Arsenic, inorganic modification, smectite, kaolinite, Freundlich isotherm, adsorption

1. Introduction

Arsenic (As) has become a major pollutant in soil and drinking water in many parts of the world. Despite being relatively scarce in the natural environment (0.0005%; 20th abundant element in the continental crust), arsenic is widely distributed over the globe (Gebreyowhannes, 2009). All over the world where arsenic contamination in groundwater and its potentially severe human health effects have been reported, the impact has been the highest in Bangladesh and the Bengal delta basin of West Bengal, India (Chowdhury et al., 2000; Mukhopadhyay et al., 2002). More than 90% of the total groundwater in West Bengal is affected by arsenic contamination (Sanyal and Nasar 2002). The contamination of water occurs due to the dissolution of minerals like arsenopyrites from parent materials, geochemical reactions, biological activities and/or from anthropogenic sources such as the leaching of manmade arsenic compounds from smelting of metal ores, and

47 wood preservatives (Shevade and Ford, 2004). There are two chemical hypotheses, namely

48 arsenopyrite oxidation hypothesis (Mandal et al., 1996) and ferric oxyhydroxide reduction

49 hypothesis (Bhattacharyya et al., 1997), which explains the widespread arsenic occurrence in the

50 groundwater of Bengal delta basin and Bangladesh. The latter hypothesis proved more consistent

51 according to some literature (Sanyal 1999; Aziz et al., 2016). According to this hypothesis, anoxic

52 condition of the aquifers caused the mobilization of arsenic from arsenic bearing minerals into the

53 groundwater.

54 Buildup of arsenic in soil due to the use of contaminated groundwater for irrigation has led to a

55 global environmental concern, especially for rice production and food security in South Asia (India

56 and Bangladesh) (Das et al., 2008; Khan et al., 2009). In addition, drinking of arsenic contaminated

57 groundwater is a direct health threat to the people in this region and other parts of the world (Liu

58 et al., 2002; Ng et al., 2003; Das et al., 2011; Sarkar et al., 2016). Consumption of arsenic

59 contaminated drinking water may cause kidney, urinary tract, liver, skin, and rectum cancers in

60 humans (Pontius, 1994). Non-carcinogenic diseases related to arsenic exposure are hypertension,

61 diabetes mellitus, cerebrovascular and cardiovascular systems, and dysfunction of respiratory

62 system (Thomas et al., 2001).

63 Arsenic is dominantly present in soils in inorganic forms which are a function of redox potential

64 and pH of the medium. Arsenate (As (V)) is the major arsenic species in surface water over the

65 pH range of 5 to 12 (Zeng, 2004). Arsenite (As (III)) is mostly found under reducing conditions,

66 and thus is the most dominant species in groundwater over the pH range of 2 to 9 (Zeng, 2004).

67 Anion exchange, adsorption, reverse osmosis, coagulation, co-precipitation and solvent extraction

68 are commonly known methods for removing arsenic from aqueous systems (Mohan and Pittman,

69 2007; Jadhav et al., 2015; Shakoor et al., 2016; Vithange et al., 2017). Various adsorbents

70   including activated carbon, biochar, agricultural and industrial byproducts, zeolite and clay

71   minerals, metal oxides and hydroxides, nanomaterials and resins were reported to remove arsenic

72   from contaminated water (Mohan and Pittman, 2007; Sharma et al., 2014). However, available

73   technologies for removing arsenic from soils are very limited. Phytoremediation of As from soil

74   could be carried out through plants such as Pteris vittata (Mandal et al., 2012; 2017; Fayiga and

75   Saha, 2016; Niazi et al., 2016). Ghosh et al. (2012) used farm yard manure and compost to make

76   chelation of arsenic with humate compounds and immobilize it in soils. While the influence of

77   organic matter on the mobility and bioavailability of arsenic species are ambiguous (Suda and

78   Makino, 2016; Wang et al., 2016), some inorganic amendments such as iron compounds,

79   phosphates, alkaline compounds, gypsum, biosolid, red mud, fly ash and clay minerals were found

80   effective in immobilizing As in soils (Lombi et al., 2004; Kumpiene et al., 2008; Miretzky and

81   Cirelli, 2010; Lee et al., 2011; Lim et al., 2016). However, many of these materials are expensive

82   and still do not have standard protocol of practical soil application.

83   Due to their low cost, worldwide distribution and superior physico-chemical properties (e.g., high

84   specific surface area, ion-exchange capacity, mechanical stability and lamellar structure), clay

85   minerals (with or without modification) have also found widespread research attention in the

86   remediation of metals and metalloids in water and soil (Sarkar et al., 2012; 2013; Sun et al., 2013;

87   Perelomov et al., 2016; Kumararaja et al., 2017). In addition, such materials are ideal for one-time

88   use requiring no regeneration.

89   Clay minerals modified with different inorganic ions like Fe, Al, Ti, organic acids, mineral acids,

90   polymers, surfactants and nanoparticles were found promising for As remediation in contaminated

91   water (Li et al., 2007; Boddu et al., 2008; Doušová et al., 2009; Akpomie and Dawodu 2016;

92   Sarkar et al., 2016). Ti-pillared smectite was considered in the present investigation due to its high

4

93 adsorption affinity towards arsenic in aqueous system as it forms a polyhydroxy stable

94 complexation with arsenic. Similarly the Fe-exchanged smectite forms stable iron-arsenate which

95 enhanced arsenic adsorption efficiency in aqueous system. However, use of these modified clay

96 minerals for the adsorption of As in contaminated soils is still an underexplored area of research.

97 There is an urgent need to develop cost-effective methods for the removal/immobilization of As

98 in contaminated soils. Therefore, the present study aimed to prepare and characterize three

99 different inorganically modified clay minerals (Fe-exchanged and Ti-pillared smectite, and

100 phosphate-bound kaolinite), and compare their As adsorption behavior in contaminated water and

101 soil.

102

103 **2. Materials and Methods**

104 2.1 Chemicals and clay minerals

105 Potassium dihydrogen phosphate (KH_2PO_4), iron sulphate heptahydrate ($FeSO_4. 7H_2O$), calcium

106 chloride dihydrate ($CaCl_2.2H_2O$) and other chemicals were of analytical grade and purchased from

107 Merck Millipore, Mumbai, India. Sodium arsenate heptahydrate ($Na_2HAsO_4.7H_2O$), and titanium

108 chloride ($TiCl_4$) were purchased from Sigma-Aldrich Chemicals Pvt. Ltd., New Delhi, India. The

109 As stock solution (1000 mgL^{-1}) was prepared using $Na_2HAsO_4.7H_2O$ in 0.01 M $CaCl_2$ in double

110 distilled water. The working solutions of As were freshly prepared by diluting the stock solution

111 in 0.01 M $CaCl_2$ solution. 0.1 N HNO_3 and 0.1 N NaOH were used to adjust the pH of As solutions

112 as necessary.

113 The smectite and kaolinite samples in the form of bentonite and kaolin were purchased respectively

114 from S D Fine-Chem Limited, Mumbai, India and Molychem, Mumbai, India. The clay samples

115 contained 88% smectite (kaolinite and quartz as impurities) and 86% kaolinite (Fe-oxides and

116 quartz as impurities), respectively, as the main mineral composition. The average particle size of

117 unmodified, Fe-exchanged and Ti-pillared smectite was 158.10, 169.30 and 174.60 nm,

118 respectively, while this values was 189.40 and 171.70 nm, respectively, for unmodified and

119 phosphate-bound kaolinite. In order to reduce the cost of production, the raw materials were used

120 as received without any purification.

121

122 2.2 Soil sample

123 Arsenic contaminated soil sample was collected (0-15 cm depth, order: Inceptisol) from Mitrapur,

124 West Bengal, India (22.9981° N and 88.6121° E). The collected soil sample was air dried under

125 shade and ground with mortar and pestle. The ground sample was passed through 2-mm sieve for

126 further analysis purposes. The As content and other physico-chemical characteristics of the soil

127 are given in Table 1.

128

129 2.3 Preparation of inorganically modified clay minerals

130 2.3.1 Preparation of iron-exchanged smectite

131 The smectite sample was treated with 0.1 M $FeSO_4$ solution in double distilled water (Te et al.,

132 2015). In brief, 20 g of dried smectite was mixed with 200 mL of 0.1 M $FeSO_4$ in a 250 mL conical

133 flask and stirred for 24 h in a mechanical shaker with a speed of 200 rpm at room temperature. The

134 solid smectite was separated using centrifugation technique (4000 rpm for 5 min) and dried at

135 105°C for 24 h. The dried smectite sample was further heated to 350°C in a muffle furnace for 3 h

136 and cooled to room temperature. Furthermore, the sample was washed with double distilled water

137 until no reddish colour appeared upon addition of 1:10 phenanthroline (negative test for Fe) and

138 dried at 60°C for overnight in a hot air oven.

139

140   2.3.2 Preparation of Ti- pillared smectite

141   At first, Na-smectite was prepared by adding 0.1 M NaOH drop by drop to a smectite suspension

142   (10% w/v) under continuous stirring in a magnetic stirrer for 16 h. The saturated particles were

143   separated through centrifugation (5000 rpm for 10 min) and washed with double distilled water

144   until it became chloride free (no white precipitation upon the addition of a drop of 0.1 N $AgNO_3$

145   solution). Then Na-smectite was dried at 80°C for 4 h for further use. Ti-pillaring of Na-smectite

146   followed the procedure of hydrolysis of $TiCl_4$ in reaction with HCl as described by Na et al. (2010).

147   In short, 100 mL of $TiCl_4$ was dissolved in 200 mL of 3 M HCl solution under vigorous stirring

148   for 2 h. The resultant solution was mixed with a 0.5 M HCl solution (1:2.5 ratio), and the pillaring

149   agent was obtained. Na-smectite (10 g) was slowly added to 490 mL of double distilled water

150   under stirring at 2000 rpm for 1 h. Then the mixture was aged for 12 h at 25°C. The pillaring agent

151   was then added into this mixture over a period of 1 h under vigorous stirring at about 3000 rpm.

152   Afterwards, the mixture was transferred to a bottle and treated in a water bath at 80°C for 6 h. The

153   product obtained was then filtered and washed with distilled water, dried, ground to powder.

154

155   2.3.3 Preparation of phosphate-bound kaolinite

156   The kaolinite sample was modified with KH_2PO_4 solution following the procedure of Amer et al.

157   (2010). Kaolinite (100 g) was equilibrated with 1 L of 200 mgL^{-1} KH_2PO_4 in a rotary orbital shaker

158   at 150 rpm for 24 h. The sample was then washed several times with double distilled water to

159   remove excess phosphate from the mineral surface. Phosphate in the washout solution was found

160   negative, and the clay sample was dried in the oven at 105°C for 24 h.

161

162   2.4 Characterization

163   The cation exchange capacity (CEC) of the clay minerals (modified and unmodified) was

164   determined by $CaCl_2$-$MgCl_2$ method (Alexiades and Jackson, 1965) and specific surface area was

165   calculated using EGME (ethylene glycol monoethyl ether) adsorption method (Heilman et al.,

166   1965).

167   X-ray diffraction analyses of the powdered samples were performed using a Philips PW1710 X-

168   ray diffractometer with a monochromatic Cu-Kα ($\lambda = 1.5418$ Å) source operating at 40 kV and 20

169   mA. The diffraction pattern recorded from 4° to 30° with a scan rate of 1.5° 2θ min^{-1}.

170   Fourier transform infra-red spectroscopy (FTIR) of the samples was carried out in the form of

171   KBr pellets using Bruker ALPHA, FTIR/ATR system (typically 64 scans, resolution 4 cm^{-1}), and

172   samples were scanned in 4,000-600 cm^{-1} region. Scanning electron microscopy (SEM) images of

173   the clay products were taken using a VEGA3 LM scanning electron microscope (Tescan Orsay

174   Holding Instrument, Czech Republic) equipped with backscattered electron (BSE) and secondary

175   electron (SE) detectors.

176   Transmission electron microscopy (TEM) images of all the modified clay products were taken

177   using a JEOL TEM model JEM-1101 (JEOL Ltd., Japan).

178

179   2.5 Adsorption studies

180   2.5.1 Adsorption kinetics

181   The kinetics of As adsorption was performed at room temperature (25±1°C) and pH 6.2

182   (maintained with 0.1 N NaOH and 0.1 N HNO_3) with an As (arsenate) concentration of 50 µg mL^{-}

183   ^{1}. Each type of unmodified and modified clay mineral (0.5 g) (solid: solution=1:20) was

184   equilibrated in triplicate with the As solution in plastic centrifuge tubes (50 mL) on an end over

185 end shaker (225 rpm). Two blanks (without adsorbent and water without As) were taken as

186 controls. The samples were equilibrated for different time intervals (20, 40, 60, 80, 100, 120, 140,

187 160 and 180 min). After equilibration, the clay samples were centrifuged at 10,000 rpm for 10 min

188 using a REMI-24 research centrifuge (REMI, Mumbai, India). The supernatant was immediately

189 filtered through 0.45-µm membrane filter. Final volume of the filtrate was made up using 2%

190 HNO$_3$ to avoid any damage to the interface on the instrument. The concentration of As in the

191 filtrate was analyzed against a standard As solution provided by the National Institute of Standards

192 and Technology (NIST) (purchased from Merck Millipore, Mumbai, India) using an inductively

193 coupled plasma mass spectrophotometer (ICP-MS) (Perkin Elmer NexION 300X, USA). The

194 amount of As adsorbed at time t (q_t) ($\mu g\ g^{-1}$) was calculated from the mass balance relationship

195 using Eq. 1:

196 $$qt = \frac{(C0 - Ct)\ v}{m} \qquad \text{(Eq. 1)}$$

197 where, C_0 and C_t are the concentrations of As ($\mu g\ mL^{-1}$) at time zero and t, respectively; v is the

198 volume of As solution (mL); and m is the mass (g) of adsorbent. At equilibration, q_t was called as

199 the equilibrium adsorption and C_t was known as the equilibrium concentration.

200

201 2.5.2 Adsorption isotherm in aqueous system

202 Various clay adsorbents (1 g) were weighed and taken in plastic centrifuge tubes (50 mL). Arsenic

203 solutions (20 mL) of various concentrations (2.5 to 50 $\mu g\ mL^{-1}$ in 0.01 M CaCl$_2$) were then added

204 into the tubes. The suspensions were equilibrated for 24 h on an end over end shaker (225 rpm) to

205 ensure the equilibrium. All the experiments were conducted in triplicate at room temperature (25

206 $\pm$ 1°C) and pH 6.2 (maintained with 0.1 N HNO$_3$ and 0.1 N NaOH). After equilibration, the

207 supernatants were separated and analyzed for As concentrations by ICP-MS as described earlier.

208   Blank tests under the same conditions revealed no As adsorption on the tube wall during the

209   reaction period. The amount of As adsorbed was calculated using Eq. 1, and the As adsorption

210   efficiency (%) was calculated using Eq. 2:

211   Adsorption efficiency (%) = $\frac{(C0-Ce)}{C0} \times 100$ (Eq. 2)

212   where, C_0 is the As concentration ($\mu g\ mL^{-1}$) at time zero; C_e is the equilibrium As concentration

213   ($\mu g\ mL^{-1}$) at time t.

214

215   2.5.3 Adsorption isotherm in soil system

216   The As contaminated soil (1.5 g) was amended with each type of clay products at 0.25% (w/w)

217   application rate in plastic centrifuge tubes. Then, 30 mL aqueous solutions of As (2.5 to 50 $\mu g\ mL^{-1}$

218   in 0.01 M CaCl$_2$) were added to the soil. Further experimental procedures and conditions were

219   maintained similar to those described earlier. All experiments were conducted in triplicate. Two

220   blank tests were conducted with soil (absence of clay products) and without soil (absence of both

221   soil and clay product). No As was adsorbed on the wall of the tubes. The amount of As adsorbed

222   by the clay products was calculated by subtracting the amount adsorbed by the soil (absence of

223   clays) from the amount adsorbed by the soil amended with the clay products using the mass balance

224   relationship (Eq. 1). Similarly, the As adsorption efficiency (%) of different clay products in the

225   soil system was calculated using Eq. 2.

226

227   2.5.4 Partition coefficient (K_d)

228   The K_d value (partition coefficient) of As adsorption on different modified clay minerals in the

229   aqueous and soil system was calculated using Eq. 3:

230                     $Kd = qe/Ce$ (Eq. 3)

231 where, K_d (mL g^{-1}) is the partition coefficient of As adsorption; q_e is the amount of As adsorbed

232 per unit mass of adsorbent at equilibrium (μg g^{-1}); C_e is the equilibrium As concentration (μg mL^{-}

233 ^{1}).

234

235 2.6 Statistical analyses

236 The kinetic and isotherm data of As adsorption were fitted to model equations (power function and

237 simple Elovich model for adsorption kinetic study, and Freundlich model for adsorption isotherm

238 study) by nonlinear regression using least squares method. The correlation coefficients (R^2)

239 obtained from the regressions analyses were used to evaluate the applicability of the model

240 equations.

241

242 **3. Results and Discussion**

243 3.1 Characterization of clay products

244 3.1.1 General properties

245 Selected physico-chemical properties of the unmodified and modified clay minerals are given in

246 Table 2. The raw smectite was alkaline in nature (pH 8.20), while the kaolinite was neutral in

247 reaction (pH 6.75). After reactions of smectite with $FeSO_4$ and $TiCl_4$, the products' pH values

248 decreased drastically to 3.93 and 5.95, respectively. This was because of saturation of the clay

249 mineral with cations (Fe^{2+} and Ti^{4+}) and also hydrolysis in the case of Ti-pillaring in the presence

250 of HCl. The pH of the kaolinite changed only slightly (pH 6.50) following the modification with

251 phosphate. The specific surface area (SSA) of the unmodified smectite was 202.69 m^2 g^{-1}, whereas

252 it had increased up to 2-folds in Fe-exchanged smectite and Ti-pillared products (485.62 and

253 437.06 m^2 g^{-1}, respectively). The SSA of kaolinite also increased by five times from 18.40 to 89.08

254    $m^2 \ g^{-1}$ after the modification with phosphate (Adebowale et al., 2006). The SSA increase in the

255   clay products was likely due to the removal of impurities from the clay minerals (Rusmin et al.,

256   2016). Additionally, the replacement of exchangeable cations, particularly with Fe^{2+} and Ti^{4+},

257   might have exposed the clay edges and increased the SSA (Akpomie and Dawodu, 2016). The

258   cation exchange capacity (CEC) of the unmodified smectite and kaolinite was 118.50 and 22.25

259   cmol (p^+) kg^{-1}, respectively, whereas the value was 115.75, 105.75 and 40.50 cmol (p^+) kg^{-1} for

260   Fe-exchanged smectite, Ti-pillared smectite and phosphate-bound kaolinite, respectively. The

261   CEC of smectite decreased after the exchange and pillaring reactions because the guest cations

262   and polyhydroxy titanium might have blocked the adsorption sites (Karamanis et al., 1997).

263   However, CEC of kaolinite was increased due to ligand adsorption of phosphate on to the clay

264   mineral surface (Ioannou and Dimirkou, 1997).

265

266   3.1.2. X-ray diffraction (XRD)

267   The XRD patterns of the unmodified and modified clay products are given in Fig. 1. The d(001)

268   value (basal spacing) was calculated from the corresponding first order reflection of the 001 plane.

269   A successful modification of the interlayer environment of the smectite was confirmed by the

270   deviation in the 2θ angle of the corresponding 001 reflection. The d(001) value of the unmodified

271   smectite was 14.24 Å (Fig. 1; Table 2) which was comparable to the d (001) value of a typical

272   montmorillonite. Both the Fe-exchanged and Ti-pillaring modifications resulted in an increase of

273   the d(001) value (interlayer expansion) (Fig. 1). The increase in d(001) value of Fe-exchanged and

274   Ti-pillared smectite was 2.11 and 2.73 Å, respectively (Table 2), which was in alignment with

275   previous reports (Karamanis et al., 1997; El Miz et al., 2014). Conversely, the d(001) values of the

276 kaolinite and phosphate-bound kaolinite were 7.25 and 7.13 Å, respectively (Fig. 1), indicating

277 that phosphate might have attached only on broken edges of the kaolinite (Bidwell et al., 1970).

278

279 3.1.3 Functional group analysis

280 The FTIR bands at 3642 and 3452 cm^{-1} (Fig. 2) in the spectra of unmodified smectite were

281 attributed to –OH bending mode of the adsorbed water (Farmer, 1974). Two other bands at 2435

282 and 1654 cm^{-1} were ascribed to the basic layer silicate structure of smectite (Madejova and

283 Komadel, 2001). The bands at 1037 and 959 cm^{-1} were due to the stretching vibration of Si-O-Si

284 groups and bending vibration of Al-O(OH)-Al groups, respectively (Madejova and Komadel,

285 2001). In the FTIR spectrum of Ti-pillared smectite (Fig. 2), the band at 3642 cm^{-1} shifted to 3696

286 cm^{-1}, and the band due to vibration of water molecules in interlayer shifted to 3397 cm^{-1} (Zhang et

287 al., 2008). Similarly, in the spectrum of Fe-exchanged smectite (Fig. 2), the band at 3642 shifted

288 to 3690 cm^{-1}, and the water molecules band moved to 3394 cm^{-1}. The shifting of bands from 3696

289 cm^{-1} to the region of 3390 cm^{-1} in both of the modified clay products suggested the H-bond

290 formation (Zhang et al., 2008). The presence of bands around 2419 cm^{-1}, 2412 cm^{-1} and 1698 cm^{-1}

291 ^{1} in both spectra of the modified clay products proved that their layer silicate structures were

292 preserved. The band around 1037 cm^{-1} indicated Si-O-Si bonding in both the modified smectites.

293 The band at 962 cm^{-1} in the spectrum of Fe-exchanged smectite confirmed the presence of Al-O-

294 Al bonding which was minimized in the case of Ti-pillared smectite. The presence of new bands

295 at 621cm^{-1} in the spectrum of Ti-pillared smectite and at 634 cm^{-1} in Fe-exchanged smectite might

296 be due to the formation of Si-O-Ti and Si-O-Fe bonds, respectively (Zhang et al., 2008). In both

297 unmodified and modified kaolinites, the appearance of the bands around 3690 and 3680 cm^{-1},

298 which were attributed to the stretching vibration of inner surface hydroxyl groups (Fig. 2)

299 (Unuabonah et al., 2008; Amer et al., 2010). The band at 3551 cm^{-1} was attributed to the OH

300 stretching vibration of inner hydroxyl group (Unuabonah et al., 2007). The band at 3551 cm^{-1} in

301 the spectrum of kaolinite was splited to 3503 and 3464 cm^{-1} in the phosphate-bound product (Fig.

302 2). The bands at 2414 and 1717 cm^{-1} in the unmodified kaolinite attributed to the typical layer

303 silicate structures and were found unchanged after the phosphate modification. The bands at 1035,

304 916 and 697 cm^{-1} in kaolinite were ascribed to Si-O-Si bond, Al-O(OH)-Al bond and Al-O bond,

305 respectively (Unuaboanh et al., 2008). Only the band for Si-O-Si bond shifted from 1035 to 1027

306 cm^{-1} after phosphate modification (Amer et al., 2010).

307

308 3.1.4 SEM characterization

309 The surface of the unmodified smectite was smooth and crystalline in structure (Fig. 3). However,

310 after modification, the Ti-pillared and Fe-exchanged smectite became swollen, fluffy and slightly

311 clustered (Akpomie and Dawodu, 2016). Swollenness and fluffiness occurred likely due to

312 increase in d(001) values of the clay mineral following modification. These changes were very

313 clear in Ti-pillared and Fe-exchanged smectite (Fig. 3). The SEM image of the unmodified

314 kaolinite was very tiny and thin plate like structural surface (Fig. 3). The kaolinite also became

315 little bit aggregated in its surface morphology after the phosphate modification (Fig. 3)

316 (Unuabonah et al., 2008).

317

318 3.1.5. TEM characterization

319 The approximate shape and size of the clay products were determined through TEM images (Fig.

320 4). The shape of smectite particle appeared as a clear crystalline structure with an approximate

321 length 41.82 nm (in one dimension) (Fig. 4). But after modification, the shapes of Ti-pillared and
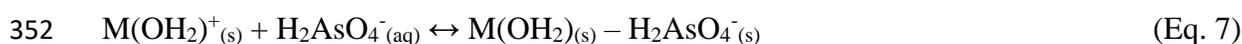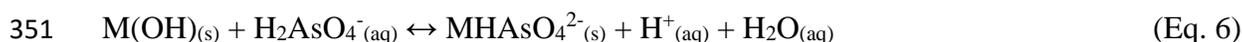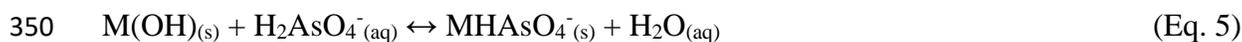
322   Fe-exchanged smectite (Fig. 4) particles became cloudy, fluffy, swollen and slightly clustered due

323   to increase in basal spacing (Seki and Yurdakoc, 2007), as was also observed in SEM images. The

324   approximate one dimensional length of Ti-pillared and Fe-exchanged smectite particles was 47.50

325   and 44.87 nm, respectively. The unmodified kaolinite particles appeared as a clear hexagonal, thin

326   plate like structure (Fig. 4) with approximate length of 275.78 nm (Ma and Eggleton, 1999). The

327   shape of phosphate-bound kaolinite (Fig. 4) did not change significantly, but remained clustered.

328   The approximate length of phosphate-bound kaolinite particle was 150.59 nm. This huge variation

329   in the length of kaolinite minerals before and after the phosphate modification might be due to

330   their irregular shaped particle distribution (Hassan and Abdu, 2014). Therefore, the TEM images

331   substantiated the SEM surface morphology results discussed earlier.

332

333   3.2. Arsenic adsorption kinetics

334   The initial adsorption of As on Ti-pillared smectite was slightly lesser than Fe-exchanged and

335   unmodified smectite (Fig. 5). The amount of As adsorbed were 448.0, 536.0 and 479.2 $\mu g g^{-1}$ by

336   Ti-pillared, Fe-exchanged and unmodified smectite at initial 20 min of adsorption (Fig. 5), which

337   suggested that Fe-exchanged smectite required less contact time to remove As from aqueous

338   system than the other two clay products. The exchanged iron (Fe) in the interlayer of smectite

339   probably formed iron hydroxides and oxides through oxidation and hydration processes during

340   reaction with water in the interlayer and the oxygen atoms at the end of each sheet of the clay

341   mineral (Stucki et al., 2002). The faster adsorption mechanism was in agreement with previous

342   reports using crystalline hydrous ferric oxide (Manna et al., 2003). Moreover, Fe had greater

343   affinity to adsorb As species than Ti (Lenoble et al., 2002). The Ti-pillared smectite started rapid

344   adsorption after a slow start. But from 40 minutes onwards, the Fe-exchanged smectite exhibited

345   more or less uniform adsorption rate and the trend continued throughout the rest of the reaction

346   period. In aqueous medium, Ti-pillared smectite adsorbed As by chemisorption mechanism

347   (Lenoble et al., 2002; Na et al., 2010). The chemisorption reaction mechanism of arsenate

348   adsorption onto Ti-pillared smectite in aqueous system is as follow:

349    $M(OH)_{(s)} + H^+ \leftrightarrow M(OH_2)^+_{(s)}$ (Eq. 4)

350    $M(OH)_{(s)} + H_2AsO_4^-{}_{(aq)} \leftrightarrow MHAsO_4^-{}_{(s)} + H_2O_{(aq)}$ (Eq. 5)

351    $M(OH)_{(s)} + H_2AsO_4^-{}_{(aq)} \leftrightarrow MHAsO_4^{2-}{}_{(s)} + H^+{}_{(aq)} + H_2O_{(aq)}$ (Eq. 6)

352    $M(OH_2)^+{}_{(s)} + H_2AsO_4^-{}_{(aq)} \leftrightarrow M(OH_2)_{(s)} - H_2AsO_4^-{}_{(s)}$ (Eq. 7)

353   where, $M(OH)_{(s)}$ represents a hydroxy group of the Ti-pillared smectite; $H^+{}_{(aq)}$ is the solution pH;

354    $MHAsO_{4(s)}$ and $MAsO_{4(s)}$ the inner sphere complex, and $M(OH_2^+) - H_2AsO_{4(s)}$ the outer sphere

355   complex of arsenate.

356   After 3 h of reaction, Fe-exchanged smectite indicated a higher As adsorption (582.8 µgg^{-1}) than

357   unmodified (530.8 µgg^{-1}) and Ti-pillared smectite (490.0 µgg^{-1}). The arsenate species ($H_2AsO_4^-$)

358   in aqueous phase is mostly dominant in between pH 2.2 to 6.98. Surface of the Fe-exchanged

359   smectite became more positively charged due to acidic nature of Fe-exchanged smectite and the

360   medium, which formed stable iron arsenate (Te et al., 2015). This might be a probable mechanism

361   of As adsorption by Fe-exchanged smectite. On the other hand, phosphate-bound kaolinite also

362   adsorbed a lesser amount of As (454.0 µgg^{-1}) than unmodified kaolinite (467.6 µgg^{-1}) initially at

363   20 min of reaction (Fig. 5), which indicated kaolinite's greater initial As removal capacity than the

364   modified product. It was likely due to the presence of some positive surface charges on broken

365   edges of the kaolinite as a function of mild acidic reaction (pH 6.2). It was reported that As

366   adsorption was regulated by its type of solution species, especially As (V) and surface charge (Xu

367   et al., 1988; Manning and Goldberg, 1996). But from 60 min onwards, unmodified kaolinite started

368   adsorbing considerably less amount than the phosphate-bound kaolinite. At equilibration,

369   phosphate-bound kaolinite adsorbed (502.2 μgg^{-1}) more than the unmodified kaolinite (495.0 μgg^{-1})

370   ). The results demonstrated that all these clay minerals and their products increased As removal

371   at equilibrium (3 h). A similar inference was drawn by several researchers (Zeng, 2004; Mohapatra

372   et al., 2007; Na et al., 2010) who used different types of smectite and kaolinite. However, among

373   all the clay minerals, Fe-exchanged smectite exhibited the maximum As adsorption (582.8 μgg^{-1})

374   and highest As removal capacity.

375   Two adsorption kinetic models (power function and simple Elovich) were used to fit the kinetic

376   data by nonlinear regression (Sparks, 1989). These models are expressed respectively by Eq. 8 and

377   9:

378   Power function equation: $q = a\, t^{b}$ (Eq. 8)

379   where, q = adsorbed As (μgg^{-1}) at time t (min); a and b are the constants; b is positive and less than

380   1.

381   Elovich equation: $q = a + b\, lnt$ (Eq. 9)

382   where, q = adsorbed As (μgg^{-1}) at time t (min); a is intercept and b is the slope. The simple Elovich

383   parameters were estimated without using the origin (q = 0, t = 0).

384   On the basis of R^2 values (>0.90), the kinetics of As adsorption onto different clay minerals could

385   be described by both the model equations (Table 3). A similar kind of inference about well fitted

386   kinetics model of As adsorption was drawn by Zeng (2004) using a Fe (III)-Si binary oxide

387   adsorbent. The higher value of 'a' in the power function equation suggested the higher adsorbed

388   amount of adsorbate with time. Similarly, in simple Elovich equation, high value of slope 'b' and

389   intercept 'a' implied higher adsorption rate with time (Sparks, 1989).

390

3.3. Adsorption isotherm study in aqueous system

The unmodified smectite was a poor adsorbent of As in aqueous system because of its low adsorption efficiency (48.56%) (Table 4). The Fe-exchanged and Ti-pillared smectites gave 73.64 and 78.82% sorption efficiency, respectively. The adsorption efficiencies were 66.07 and 79.05% in unmodified kaolinite and phosphate-bound kaolinite, respectively. High adsorption efficiency of modified smectite can be explained by high specific surface area and more availability of exchangeable sites. Earlier, Grygar et al. (2007) reported that As adsorption was enhanced due to the presence of high amount of Fe in Fe-exchanged smectite. Ti-pillared smectite gave the highest adsorption efficiency among all the smectites. Owing to the expansion of the interlayer after Ti-pillaring. The polyhydroxy titanium cations led to the generation of many active OH^- ions. Later on, As species formed complexation with OH^- ions of smectite in the aqueous system (Na et al., 2010). The adsorption efficiency of unmodified kaolinite was higher than unmodified smectite. The edges of kaolinite might have provided some positive surface charges due to the presence of mild acidic aqueous medium (pH 6.2) and As could form an aqua complexation (Mohapatra et al., 2007). The phosphate-bound kaolinite accounted for higher adsorption efficiency likely due to its higher surface area and the ligand exchange between phosphate and solution As species. Like the adsorption efficiency, average partition coefficient [K_d (mLg^{-1})] followed a similar trend. The Ti-pillared smectite exhibited the maximum K_d value (175.77) followed by Fe-exchanged smectite (121.89), phosphate-bound kaolinite (109.46), unmodified kaolinite (85.20) and unmodified smectite (67.30) (Table 4). Ramesh et al. (2007) reported that the K_d value increased for As adsorption because of the increased surface area and availability of more exchangeable sites in polymeric Fe-modified montmorillonite. Therefore, variations in K_d values of different modified clay products might be supported by the reasons explained for the adsorption efficiencies. Simply,

414   higher the sorption efficiency, higher is the partition coefficient. However, in general, with the

415   increasing equilibrium concentration of As, the adsorption amount decreased onto the clay

416   products in the aqueous system.

417   Freundlich adsorption isotherm has more flexibility. Any changes in adsorption behavior can be

418   best described by Freundlich isotherm. Data for As adsorption onto different clay minerals in

419   aqueous system (Fig. 6) was fitted to the Freundlich isotherm model only (Eq. 10) due to surface

420   heterogeneity of the modified clays and high significant coefficient of determination (R^2).

421                                $q = K\,C^{1/n}$ (Eq. 10)

422   where, q is the amount of adsorbed As on different clay minerals at equilibrium (μgg^{-1}), and C is

423   the As equilibrium concentration in solution ($\mu g\ mL^{-1}$), K and (1/n) are the Freundlich constants.

424   K represents the adsorption of As at equilibrium concentrations, and (1/n) indicates the degree to

425   which adsorption is a function of As concentration (Table 5).

426   The 1/n values signify the degree of the intensity of adsorption. The 1/n values for As adsorption

427   on the modified clay minerals were less than unity indicating L-type isotherms (Giles et al., 1960).

428   L-type isotherms are characterized by the decrease in the adsorption at higher aqueous

429   concentrations of the solute. This suggests a greater competition for adsorption sites which become

430   limited as solute concentration in solution increases.

431   To obtain a meaningful comparison of their K values, the 1/n values for all modified clay minerals

432   should nearly be equivalent. The K (μgg^{-1}) value or As adsorption capacity was the maximum in

433   Ti-pillared smectite (156.54), followed by Fe-exchanged smectite (127.63), phosphate-bound

434   kaolinite (124.43), unmodified kaolinite (93.82) and unmodified smectite (66.03). The higher K

435   value might be explained by the respective K_d values. The higher partition coefficient (K_d)

436   suggested higher As adsorption capacity (K) by the modified clay products. The other reason might

437   be the surface complexation which is one of the stable bond formations that occurred in the case

438   of Ti-pillared smectite. The R^2 obtained for Freundlich model fitting were more than 0.90 for all

439   modified clays except the unmodified smectite and kaolinite (Table 5). Arsenate and arsenite

440   adsorption on iron oxide-coated sand and ferrihydrite was also best described earlier by the

441   Freundlich isotherm model (Thirunavukkarasu et al., 2001). The Freundlich isotherm model fitted

442   the experimental data very well due to the heterogeneous distribution of active sites on the

443   modified clay mineral surfaces. The 1/n values of all the clay minerals were less than 1 (Table 5),

444   which suggested that the adsorption process was favorable (Treybal, 1980). Similar results of

445   Freundlich model fitting and 1/n values less than unity for the adsorption of As (V), As (III) and

446   organic As species on polymeric Al/Fe-modified montmorillonite was reported by Ramesh et al.

447   (2007). Among all the smectites, Ti-pillared smectite adsorbed the maximum amount of As,

448   followed by Fe-exchanged and unmodified smectite (Fig. 6). The phosphate-bound kaolinite

449   adsorbed more As than unmodified kaolinite (Fig. 6). The reason might be that As has more spatial

450   compatibility with the adsorption sites of modified clay minerals because of their high surface

451   area. Therefore, the highest As adsorption capacity (K) onto the modified clay minerals in aqueous

452   system maintained the order: Ti-pillared smectite > Fe-exchanged smectite > phosphate-bound

453   kaolinite > unmodified kaolinite > unmodified smectite.

454

455   3.4 Adsorption isotherm study in soil system

456   Very few studies so far focused on the adsorption of As by modified clay minerals in contaminated

457   soils (Sarkar et al., 2012). The adsorption behavior of different modified clay minerals in the soil

458   system was slightly different from that of the aqueous system (Table 4). The adsorption

459   efficiencies were in the order: Fe-exchanged smectite > Ti-pillared smectite > phosphate-bound

460 kaolinite > unmodified kaolinite > unmodified smectite (Table 4). The maximum adsorption

461 efficiency of the Fe-exchanged smectite could be explained by higher surface area and higher

462 positive charge of Fe-exchanged smectites due to reduction in pH (Table 2). Similarly, the

463 increased surface area and ligand exchange reaction imparted greater adsorption efficiency by

464 phosphate-bound kaolinite than the unmodified kaolinite. Phosphate and arsenate ions could

465 compete non-specifically for ligand exchange and complexation sites on kaolinite when present

466 simultaneously in the soil system (Goldberg, 2002). But following modification with phosphate,

467 the kaolinite adsorbed more As than the unmodified counterpart. Earlier, Violante and Pinga

468 (2002) also reported a higher affinity of kaolinite to adsorb arsenate than phosphate. The

469 adsorption mechanism of Ti-pillared smectite would be the same as discussed in the aqueous

470 system. Partition coefficient [K_d (mLg^{-1})] values also followed the same trend of adsorption

471 efficiencies (Table 4). The Fe-exchanged smectite had the maximum K_d (100.13) value (Table 4).

472 However, adsorption efficiencies (except in unmodified smectite) and K_d values for all clay

473 products became lower in the soil system than the aqueous system because the former system was

474 more heterogeneous than the latter. In soil system several factors (e.g., clay type and content,

475 amorphous Fe content, total Fe content, soil pH and organic carbon) (Table 1) (Rivaz-Perez et al.,

476 2015) along with competitive ions might have influenced arsenic adsorption behavior on modified

477 clay minerals.

478 Arsenic adsorption data in the soil system were also fitted to the Freundlich equation (Eq. 10)

479 having $R^2 > 0.85$. Like the aqueous system, here also the 1/n values were less than unity (Table 5).

480 The Freundlich coefficient K (μgg^{-1}) was the highest in Fe-exchanged smectite (115.63) followed

481 by other clay products and maintained the same trends of adsorption efficiency and partition

482 coefficient (K_d) (Table 5). The pH of contaminated soil was 6.49, which was almost equal to the

483   pH value (6.2) maintained in the solid-solution interaction experiment. Mohapatra et al. (2007)

484   reported that montmorillonite and kaolinite adsorbed the maximum amount of arsenate at pH 6.0

485   and 5.0, respectively. As a result, the modified kaolinite accounted for a lesser K value for As

486   adsorption than the modified smectite.

487   Fig. 7 depicted some irregular or discontinuous adsorption trend followed in the soil system. With

488   the increase in solute concentration, there were breaks and reverse turns in the adsorption curves

489   for both smectite and kaolinites. The Fe-exchanged smectite and unmodified kaolinite exhibited a

490   more continuous increasing trend of adsorption than the other clay products (Fig. 7). The

491   deviations were greater at relatively higher equilibrium concentration of As. Ti-pillared smectite,

492   unmodified smectite and phosphate-bound kaolinite started showing the reverse breaks after 14.3,

493   22.74 and 12.11 $\mu g\ mL^{-1}$ equilibrium concentrations, respectively. This discontinuous trend of

494   solute concentration could be explained by the formation of binuclear As complexes and As

495   precipitation in the soil system (Datta 2002). In a similar fashion, phosphorus solution

496   concentration sharply decreased after attaining a maximum value due to the precipitation of

497   phosphorus in soil (Datta 2002). The non-labile P formation took place due to binuclear complex

498   formation and precipitation (Datta 2002). The precipitated phosphorus became crystallized and

499   non-labile with time (Datta 2002). Arsenic is also analogous to phosphorus (Marschner, 1995),

500   and probably followed the same mechanism in the soil system. Therefore, binuclear complexes

501   and precipitation might have taken place on the surfaces of these modified clay products in soil as

502   a function of soil constituents and competitive anions. Thus, precipitation or binuclear complex

503   formation of As by these modified clay products was quite effective to immobilize As from labile

504   form to non-labile form in the soil.

505

4. Conclusions

Modifications of smectite and kaolinite through Fe-exchange, Ti-pillaring and phosphate binding were confirmed by XRD, FTIR, SEM and TEM characterization techniques. The smectite products (Fe-exchanged and Ti-pillared) were more efficient in As adsorption than phosphate-bound kaolinite in both soil and aqueous systems. While the Ti-pillared smectite was the most suitable product for As adsorption in the aqueous system due to surface complex formation, the Fe-exchanged smectite showed the best effectiveness in the soil system because of its high surface area ($485.62 \ m^2 \ g^{-1}$) and higher affinity to As. The phosphate-bound kaolinite adsorbed As to a greater extent than unmodified kaolinite through ligand exchange mechanism in both the systems. One of the most important properties exhibited by some of the clay minerals was As precipitation and/or binuclear complex formation in the soil system. This made As non-labile in soil with time passed, which was most desirable and effective in remediating the metalloid. Thus, the application of these modified clay products hold a great potential to immobilize As not only in contaminated groundwater and drinking water, but also in contaminated soil.

23

529   **References**

530   Adebowale, K.O.; Unuabonah, E.I.; Olu-Owolabi, B.I., 2006. The effect of some operating

531   variables in the adsorption of lead and cadmium ions on kaolinite clay. J. Hazard. Mater.

532   134, 130-139.

533   Akpomie, K. G.; Dawodu, F.A., 2016. Acid-modified montmorillonite for sorption of heavy

534   metals from automobile effluents. Beni-Suef Univ. J. Appl. Sci. 5, 1-12.

535   Alexiades, C.A.; Jackson, M. L., 1965. Quantitative determination of vermiculite in soils. Soil Sci.

536   Soc. Am. Proc. 29, 522-527.

537   Amer, M.; Khalili, F.; Awad, A., 2010. Adsorption of lead, zinc and cadmium ions on

538   polyphosphate-modified kaolinite clay. J. Env. Chem. Ecotoxicol. 2, 1-8.

539   Aziz, Z.; Bostick, B.C.; Zheng, Y.; Huq, M.R.; Rahman, M.M.; Ahmed, K.M.; Van Geen, A.,

540   2016. Evidence of decoupling between arsenic and phosphate in shallow groundwater of

541   Bangladesh   and   potential   implications.   Appl.   Geochem.   1-11,

542   http://dx.doi.org/10.1016/j.apgeochem.2016.03.001.

543   Bhattacharyya, P.; Chatterjee, D.; Jacks, G., 1997. Occurrence of arsenic contaminated

544   groundwater in alluvial aquifers from delta plains, Eastern India: Options for safe drinking

545   water supply. Int. J. Water Res. Dev. 13, 79- 92.

546   Bidwell, J. I.; Jepson, W.B.; Toms, G.L., 1970. The interaction of kaolinite with poly-phosphate

547   and polyacrylate in aqueous solutions-some preliminary results. Clay Miner. 8, 445-459.

548   Boddu, V.M.; Abburi, K.; Talbott, J.L.; Smith, E.D.; Haasch, R., 2008. Removal of arsenic (III)

549   and arsenic (V) from aqueous medium using chitosan-coated biosorbent. Water Res. 42,

550   633-642.

24

551 Chowdhury, U.K.; Biswas, B.K.; Chowdhury, T.R.; Samanta, G.; Mandal, B.K.; Basu, G.K.;

552   Chanda, C.R.; Lodh, D.; Saha, K.C.; Mukherjee, S.C.; Roy, S.; Kabir, S.; Ouamruzzaman,

553   Q.; Chakraborti, D., 2000. Groundwater arsenic contamination in Bangladesh and West

554   Bengal, India. Env. Health. Persp. 108, 393-397.

555 Das, D.K.; Sur, P.; Das, K., 2008. Mobilisation of arsenic in soils and in rice (Oryza sativa L.)

556   plants affected by organic matter and zinc application in irrigation water contaminated with

557   arsenic. Plant Soil. Env. 54, 30–37.

558 Das, I.; Ghosh, K.; Das, D.K.; Sanyal, S.K., 2011. Studies on fractionation of Arsenic in soil in

559   relation to crop uptake. Soil. Sediment Contam. 20, 790-809.

560 Datta, S.C., 2002. Threshold levels of release and fixation of phosphorus: Their nature and method

561   of determination. Commun. Soil Sci. Plant Anal. 33, 213-227.

562 Doušová, B.; Fuitová, L.; Grygar, T.; Machovič, V.; Koloušek, D.; Herzogová, L.; Lhotka, M.,

563   2009. Modified aluminosilicates as low-cost sorbents of As(III) from anoxic groundwater.

564   J. Hazard. Mater. 165, 134-140.

565 El Miz, M.; Sahil, S.; Chraibi, I.; El Bachiri, A.; Fauconnier, M.L.; Tahani, A., 2014.

566   Characterization and adsorption of pillared bentonite. Open J. Phys. Chem. 4, 98-116.

567 Farmer, V. C., 1974. The layer silicates. In: Farmer, V. C (Eds.), The infrared spectra of minerals,

568   Mineralogical Society Monograph 4. London, pp. 331–363.

569 Fayiga, A.O.; Saha, U.K., 2016. Arsenic hyper accumulating fern: Implications for remediation of

570   arsenic contaminated soils. Geoderma. 284, 132-143.

571 Gebreyowhannes, Y. B., 2009. Effect of silica and pH on arsenic removal by iron-oxide coated

572   sand. M.Sc. Thesis, UNESCO-IHE Institute for Water Education, Delft, The Netherlands.

573   Ghosh, K.; Das, I.; Das, D.K.; Sanyal, S.K., 2012. Evaluation of humic and fulvic acid extracts of

574   compost, oilcake, and soils on complex formation with arsenic. Soil Res. 50, 239-248.

575   Giles, C. H.; McEvans, T. H.; Nakhwa, S. N.; Smith, D., 1960. Studies in adsorption. Part XI: a

576   system of classification of adsorption isotherms and its use in diagnosis of adsorption

577   mechanism and measurement of specific surface areas of solids. J. Chem. Soc. 4, 3973–

578   3993.

579   Goldberg, S., 2002. Competitive adsorption of Arsenate and Arsenite on oxides and clay minerals.

580   Soil Sci. Soc. Am. J. 66, 413-421.

581   Grygar, T.; Hradil, D.; Bezdicka, P.; Dousova, B.; Capek, L.; Schneeweiss, O., 2007. Fe(III)

582   modified montmorillonite and bentonite: Synthesis, chemical and UV-vis spectral

583   characterization, arsenic sorption, and catalysis of oxidative dehydrogenation of propane.

584   Clays Clay Miner. 55, 165-176.

585   Hassan, U.J.; Abdu, S.G., 2014. Structural analysis and surface morphology of kaolin. Sci. World

586   J. 9, 33-37.

587   Heilman, M.D.; Carter, D.L.; Gonzalez, C.L., 1965. The ethylene glycol monoethyl ether (EGME)

588   technique for determining soil surface area. Soil Sci. 100, 409-413.

589   Ioannou, A.; Dimirkou, A., 1997. Phosphate adsorption on hematite, kaolinite, and kaolinite–

590   hematite (k–h) systems as described by a constant capacitance model. J. Colloid Interface

591   Sci. 192, 119-128.

592   Jadhav, S.V.; Bringas, E.; Yadav, G.D.; Rathod, V.K.; Ortiz, I.; Marathe, K.V., 2015. Arsenic and

593   fluoride contaminated groundwaters: A review of current technologies for contaminants

594   removal. J. Environ. Manage. 162, 306-325.

595   Karamanis, D.T.; Aslanoglou, X.; Assimakopoulos, P.A.; Gangas, N.H.; Pakou, A.; Papayanakos,

596   N., 1997. An aluminium pillared montmorillonite with fast uptake of cesium and strontium

597   from aqueous system. Clays Clay Miner. 45, 709-717.

598   Khan, M.A.; Islam, M. R.; Panaullah, G.M.; Duxbury, J.M.; Jahiruddin, M.; Loeppert, H., 2009.

599   Fate of irrigation water arsenic in rice soils of Bangladesh. Plant Soil. 322, 263–277.

600   Kumararaja, P.; Manjaiah, K.M.; Datta, S.C.; Sarkar, B., 2017. Remediation of metal contaminated

601   soil by aluminium pillared bentonite: Synthesis, characterisation, equilibrium study and

602   plant growth experiment. Appl. Clay Sci. 137, 115-122.

603   Kumpiene, J.; Lagerkvist, A.; Maurice, C., 2008. Stabilization of As, Cr, Cu, Pb and Zn in soil

604   using amendments – A review. Waste Manage. 28, 215-225.

605   Lee, S.-H.; Kim, E.Y.; Park, H.; Yun, J.; Kim, J.-G., 2011. In situ stabilization of arsenic and

606   metal-contaminated agricultural soil using industrial by-products. Geoderma 161, 1-7.

607   Lenoble, V.; Bouras, O.; Deluchat, V.; Serpaud, B.; Bollinger, J., 2002. Arsenic adsorption onto

608   pillared clays and iron oxides. J. Colloid Interface Sci. 255, 52-58.

609   Li, Z.; Beachner, R.; Mcmanama, Z.; Hanlie, H., 2007. Sorption of arsenic by surfactant-modified

610   zeolite and kaolinite. Micropor. Mesopor. Mat. 105, 291-297.

611   Lim, J.E.; Sung, J.K.; Sarkar, B.; Wang, H.; Hashimoto, Y.; Tsang, D.C.W.; Ok, Y.S., 2016.

612   Impact of natural and calcined starfish (Asterina pectinifera) on the stabilization of Pb, Zn

613   and As in contaminated agricultural soil. Environ. Geochem. Health. 1-11,

614   doi:10.1007/s10653-016-9867-4.

615   Liu, J.; Zheng, B.S.; Aposhian, H.V.; Zhou, Y.S.; Chen, M.L.; Zhang, A.H.; Waalkes, M.P., 2002.

616   Chronic arsenic poisoning from burning high-arsenic-containing coal in Guizhou, China.

617   Environ. Health Perspect. 110, 119-122.

618 Lombi, E.; Hamon, R.E.; Wieshammer, G.; McLaughlin, M.J.; McGrath, S.P., 2004. Assessment

619   of the use of industrial by-products to remediate a copper- and arsenic-contaminated Soil.

620   J. Environ. Qual. 33, 902-910.

621 Ma, C.; Eggleton, R.A., 1999. Surface layer types of kaolinite: A high resolution transmission

622   electron microscope study. Clays Clay Miner. 47, 181-191.

623 Madejová, J.; Komadel, P., 2001. Baseline studies of the clay minerals society source clays:

624   Infrared methods. Clays Clay Miner. 49, 410-432.

625 Mandal, B.K.; Chowdhury, T.R.; Samanta, G.; Basu, G.K.; Chowdhury, P.P.; Chanda, C.R.; Lodh,

626   D.; Naran, N.K.; Dhara, R.K.; Tamili, D.K.; Das, D.; Saha, K.C.; Chakraborti, D., 1996.

627   Arsenic in groundwater in seven districts of West Bengal, India – the biggest arsenic

628   calamity in the world. Curr. Sci. 70, 976- 986.

629 Mandal, A.; Purakayastha, T.J.; Patra, A.K.; Sanyal, S.K., 2012. Phytoremediation of arsenic

630   contaminated soil by Pteris vittata L. II. Effect on arsenic uptake and rice yield. Int. J.

631   Phytoremediation. 14, 621-628.

632 Mandal, A.; Purakayastha, T.J.; Patra, A.K.; Sarkar, B., 2017. Arsenic phytoextraction by Pteris

633   vittata improves microbial properties in contaminated soil under various phosphate

634   fertilizations. Appl. Geochem. doi: 10.1016/j.apgeochem.2017.04.008.

635 Manna, B. R.; Dey, S.; Debnath, S.; Ghosh, U. C., 2003. Removal of arsenic from groundwater

636   using crystalline hydrous ferric oxide (CHFO). Water Qual. Res. J. Can. 38, 193–210.

637 Manning, B. A.; Goldberg, S., 1996. Modeling arsenate competitive adsorption on kaolinite,

638   montmorillonite and illite. Clays Clay Miner. 44, 609-623.

639 Marschner, H., 1995. Mineral Nutrition of Higher Plants. Academic Press, New York.

640 Miretzky, P.; Cirelli, A.F., 2010. Remediation of arsenic-contaminated soils by iron amendments:

641   A review. Crit. Rev. Env. Sci. Technol. 40, 93-115.

642 Mohan, D.; Pittman Jr, C.U., 2007. Arsenic removal from water/wastewater using adsorbents- A

643   critical review. J. Hazard. Mater. 142, 1-53.

644 Mohapatra, D.; Mishra, D.; Roy Chaudhury, G.; Das, R. P., 2007. Arsenic adsorption mechanism

645   on clay minerals and its dependence on temperature. Korean J. Chem. Eng. 24, 426-430.

646 Mukhopadhyay, D.; Mani, P.K.; Sanyal, S.K., 2002. Effect of phosphorus, arsenic and farmyard

647   manure on arsenic availability in some soils of West Bengal. J. Ind. Soc. Soil Sci. 50, 56-

648   61.

649 Na, P.; Jia, X.; Yuan, B.; Li, Y.; Na, J.; Chen, Y.; Wang, L., 2010. Arsenic adsorption on Ti-

650   pillared montmorillonite. J. Chem. Technol. Biot. 85, 708-714.

651 Niazi, N.K.; Bashir, S.; Bibi, I.; Murtaza, B.; Shahid, M.; Javed, M.T.; Shakoor, M.B.; Saqib, Z.A.;

652   Nawaz, M.F.; Aslam, Z.; Wang, H.; Murtaza, G., 2016. Phytoremediation of arsenic-

653   contaminated soils Using Arsenic hyper accumulating ferns. In: Ansari, A.A.; Gill, S.S.;

654   Gill, R.; Lanza, G.R.; Newman, L. (Eds.). Phytoremediation: Management of

655   Environmental Contaminants, Volume 3. Springer International Publishing, Cham, pp. 521-

656   545.

657 Ng, J.C.; Wang, J.; Shraim, A., 2003. A global health problem caused by arsenic from natural

658   sources. Chemosphere. 52, 1353-1359.

659 Perelomov, L.; Sarkar, B.; Rahman, M.M.; Goryacheva, A.; Naidu, R., 2016. Uptake of lead by

660   Na-exchanged and Al-pillared bentonite in the presence of organic acids with different

661   functional groups. Appl. Clay Sci. 119, Part 2, 417-423.

662 Pontius, F.W., 1994. Crafting a new arsenic rule. J. Am. Water Works Assoc. 86, 6.

663   Ramesh, A.; Hasegawa, H.; Maki, T.; Ueda, K., 2007. Adsorption of inorganic and organic arsenic

664   from aqueous solutions by polymeric Al/Fe modified montmorillonite. Sep. Purif Technol.

665   56, 90-100.

666   Rivaz-Perez, I.M.; Paradelo-Nunez, R.; Novoa-Munoz, J.C.; Arias-Estevez, M.; Fernandez-

667   Sanjurjo, M.J.; Álvarez-Rodríguez, E.; Núñez-Delgado, A., 2015. As(V) and P competitive

668   sorption on soils, by-products and waste materials. Int. J. Environ. Res. Public Health. 12,

669   15706-15715.

670   Rusmin, R.; Sarkar, B.; Biswas, B.; Churchman, J.; Liu, Y.; Naidu, R., 2016. Structural,

671   electrokinetic and surface properties of activated palygorskite for environmental

672   application. Appl. Clay Sci. 134, Part 2, 95-102.

673   Sanyal, S.K., 1999. Chemodynamics of geogenic contaminants in the soil environment-Arsenic.

674   In: Proceedings of the Second International. Conference on Contaminants in the Soil

675   Environment in the Australasia-Pacific Region, New Delhi, December 12-17, 1999.

676   Extended Abstracts, pp. 389-390. Indian Network for Soil Contamination Research, New

677   Delhi, India and Soil Contamination Research in Asia and the Pacific, Adelaide, Australia.

678   Sanyal, S.K.; Nasar, S.K.T., 2002. Arsenic contamination of groundwater in West Bengal (India):

679   build-up in soil-crop system. In 'Analysis and practice in water resources engineering for

680   disaster mitigation'. Volume 1. Indian Association of Hydrologists. pp. 216–222. (New Age

681   International Publishers: New Delhi).

682   Sarkar, A.; Paul, B., 2016. The global menace of arsenic and its conventional remediation - A

683   critical review. Chemosphere. 158, 37-49.

684   Sarkar, B.; Naidu, R.; Megharaj, M., 2013. Simultaneous adsorption of tri- and hexavalent
685   chromium by organoclay mixtures. Water Air Soil Pollut. 224, 1704, doi: 10.1007/s11270-
686   013-1704-0.

687   Sarkar, B.; Naidu, R.; Rahman, M.M.; Megharaj, M.; Xi, Y., 2012. Organoclays reduce arsenic
688   bioavailability and bio accessibility in contaminated soils. J. Soils Sediments. 12, 704-712.

689   Seki, Y.; Yurdakoc, K., 2007. Identification and characterization of Fe-rich smectites in the Ç
690   amlıca Region of western Turkey. Clay Miner. 42, 153-160.

691   Shakoor, M.B.; Niazi, N.K.; Bibi, I.; Murtaza, G.; Kunhikrishnan, A.; Seshadri, B.; Shahid, M.;
692   Ali, S.; Bolan, N.S.; Ok, Y.S.; Abid, M.; Ali, F., 2016. Remediation of arsenic-contaminated
693   water using agricultural wastes as biosorbents. Crit. Rev. Env. Sci. Technol. 46, 467-499.

694   Sharma, A.K.; Tjell, J.C.; Sloth, J.J.; Holm, P.E., 2014. Review of arsenic contamination, exposure
695   through water and food and low cost mitigation options for rural areas. Appl Geochem. 41,
696   11-33.

697   Shevade, S.; Ford, R.G., 2004. Use of synthetic zeolites for arsenate removal from pollutant water.
698   Water Res. 38, 3197-3204.

699   Sparks, D. L., 1989. Kinetics of soil chemical processes. Academic Press, Inc., New York.

700   Stucki, J.W.; Lee, K.; Zhang, L.; Larson, R.A., 2002. Effects of iron oxidation state on the surface
701   and structural properties of smectites. Pure Appl. Chem. 74, 2145-2158.

702   Suda, A.; Makino, T., 2016. Effect of organic amendments on arsenic solubilization in soils during
703   long-term flooded incubation. Int. J. Env. Sci. Technol. 13, 2375-2382.

704   Sun, Y.; Sun, G.; Xu, Y.; Wang, L.; Liang, X.; Lin, D., 2013. Assessment of sepiolite for
705   immobilization of cadmium-contaminated soils. Geoderma. 193–194, 149-155.

706 Te, B.; Wichitsathian, B.; Yossapol, C., 2015 Modification of natural common clays as low cost

707   adsorbents for arsenate adsorption. Int. J. Env. Sci. Dev. 6, 799-804.

708 Thirunavukkarasu, O.S.; Viraraghavan, T.; Subramanian, K.S., 2001. Removal of arsenic in

709   drinking water by iron oxide-coated sand and ferrihydrite - batch studies. Wat. Qual. Res.

710   J. Can. 36, 55–70.

711 Thomas, D. J.; Styblo, M.; Lin, S., 2001. The cellular metabolism and systemic toxicity of arsenic.

712   Toxicol. Appl. Pharm. 176, 127-144.

713 Treybal, R.E., 1980. Mass Transfer Operations, third ed., McGraw-Hill, New York.

714 Unuaboanh, E.I.; Adebowale, K.O; Olu-owalabi, B.I., 2007. Kinetic and thermodynamic studies

715   for adsorption of lead (II) ions onto phosphate- modified kaolinite clay. J. Hazard. Mater.

716   144, 386-395.

717 Unuaboanh, E.I.; Olu-owalabi, B.I.; Adebowale, K.O.; Yang, L.Z., 2008. Removal of lead and

718   cadmium Ions from aqueous solution by polyvinyl alcohol-modified kaolinite clay: A novel

719   nano-clay adsorbent. Adsorpt. Sci. Technol. 26, 383-405.

720 Violante, A.; Pinga, M., 2002. Competitive sorption of srsenate and phosphate on different

721   clay minerals and soils. Soil Sci. Soc. Am. J. 66, 1788-1796.

722 Vithanage, M.; Herath, I.; Joseph, S.; Bundschuh, J.; Bolan, N.; Ok, Y.S.; Kirkham, M.B.;

723   Rinklebe, J., 2017. Interaction of arsenic with biochar in soil and water: A critical review.

724   Carbon. 113, 219-230.

725 Wang, P.; Liu, Y.; Menzies, N.W.; Wehr, J.B.; de Jonge, M.D.; Howard, D.L.; Kopittke, P.M.;

726   Huang, L., 2016. Ferric minerals and organic matter change arsenic speciation in copper

727   mine tailings. Environ. Pollut. 218, 835-843.

728   Xu, H.; Allard, B.; Grimvall, A., 1988. Influence of pH and organic substance on the adsorption

729   of As(V) on geologic materials. Water Air Soil Pollut. 40, 293-305.

730   Zeng, L., 2004. Arsenic adsorption from aqueous solutions on an Fe(III)-Si binary oxide adsorbent.

731   Water Qual. Res. J. Can. 39, 267-275.

732   Zhang, Y.; Song, S.; Zhang, M., 2008. Preparation and characterization of titanium - pillared

733   montmorillonite. Surf. Rev. Lett. 15, 329-336.

734

Tables

Table 1: Physico-chemical properties of arsenic contaminated soil (Mitrapur, West Bengal, India)

Properties	Values
Clay (%)	26.5
Sand (%)	23.2
Silt (%)	50.3
Textural Class	Silty clay loam
pH (1:2.5)	6.49
EC (dS m^{-1})	0.26
Organic carbon (g kg^{-1})	4.50
Amorphous Fe (%)	0.29
Total Fe (%)	1.31
Total As (mg kg^{-1})	14.1
Olsen extractable As (mg kg^{-1})	3.6
CEC [cmol (p$^+$) kg^{-1}]	24.7

Table 2: Characteristics of unmodified and modified clay minerals

Clay minerals	pH (1:2.5)	Specific surface area (m^2 g^{-1})	Cation exchange capacity [cmol (p$^+$) kg^{-1}]	d(001) (Å)
Unmodified smectite	8.20	202.69	118.50	14.24
Fe-exchanged smectite	3.93	485.62	115.75	16.35
Ti-pillared smectite	5.95	437.06	105.75	16.97
Unmodified kaolinite	6.75	18.40	22.25	7.25
Phosphate-bound kaolinite	6.50	89.08	40.50	7.13

Table 3: Estimated kinetic model parameters for arsenic adsorption on unmodified and modified clay minerals in aqueous medium

Models	Parameter	Ti-pillared smectite	Fe-exchanged smectite	Unmodified smectite	Phosphate-bound kaolinite	Unmodified kaolinite
Power function	a	398.66	475.78	408.56	397.2	435.18
	b	0.039	0.038	0.051	0.047	0.026
	R^2	0.92	0.95	0.97	0.98	0.96
Simple Elovich	a	392.88	469.12	398.2	389.43	432.76
	b	18.31	21.04	25.56	22.35	12.48
	R^2	0.92	0.94	0.97	0.98	0.96

The initial As addition was 50 µg As mL^{-1}, solid: solution = 1: 20, and pH maintained at 6.2

Table 4: Average partition coefficient (K_d) and adsorption efficiency of arsenic for different unmodified and modified clay minerals in aqueous and soil systems

Clays	K_d (mL g^{-1}) in aqueous system	K_d (mL g^{-1}) in soil system	Adsorption efficiency in aqueous system (%)	Adsorption efficiency in soil system (%)
Unmodified smectite	67.30	47.15	48.56	53.80
Fe-exchanged smectite	121.89	100.13	73.64	72.08
Ti-pillared smectite	175.77	85.45	78.82	68.58
Unmodified kaolinite	85.20	54.48	66.07	58.36
Phosphate-bound kaolinite	109.46	70.70	79.05	66.90

Table 5: Freundlich isotherm model constants for arsenic adsorption on different unmodified and modified clay minerals in aqueous and soil systems

Adsorption system	Parameters	Ti-pillared smectite	Fe-exchanged smectite	Unmodified smectite	Phosphate-bound kaolinite	Unmodified kaolinite
Aqueous	K (µg/g $(mL/µg)^{1/n}$)	156.54	127.63	66.03	124.43	93.82
	1/n	0.46	0.46	0.39	0.62	0.50
	R^2	0.91	0.93	0.48	0.92	0.65
Soil	K (µg/g $(mL/µg)^{1/n}$)	104.19	115.63	65.54	95.05	68.65
	1/n	0.48	0.49	0.46	0.49	0.53
	R^2	0.86	0.85	0.63	0.85	0.66

Figures
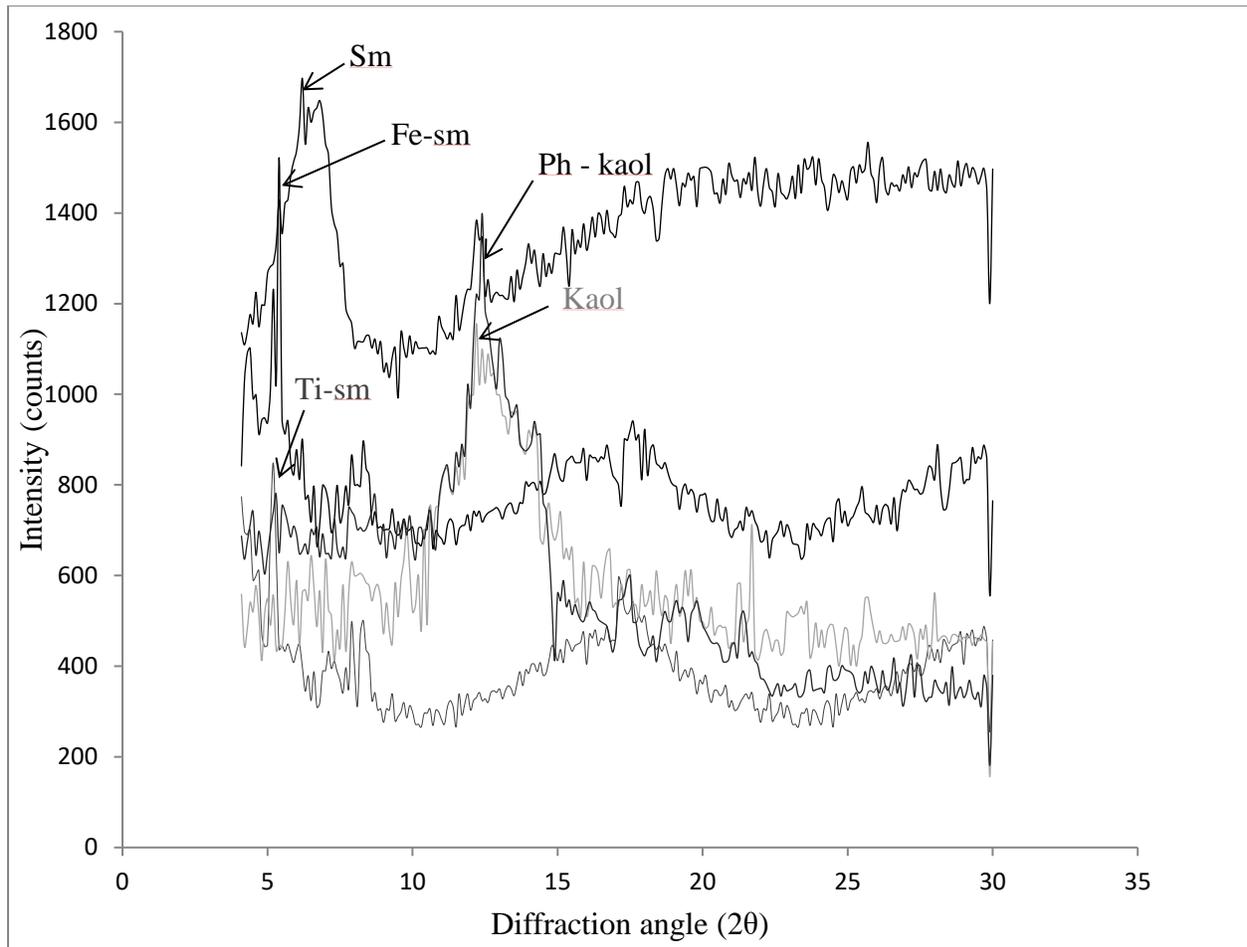
Fig. 1 X-ray diffraction patterns of unmodified smectite (Sm), Ti-pillared smectite (Ti-sm), Fe-exchanged smectite (Fe-sm), unmodified kaolinite (Kaol) and phosphate-bound kaolinite (Ph-kaol)
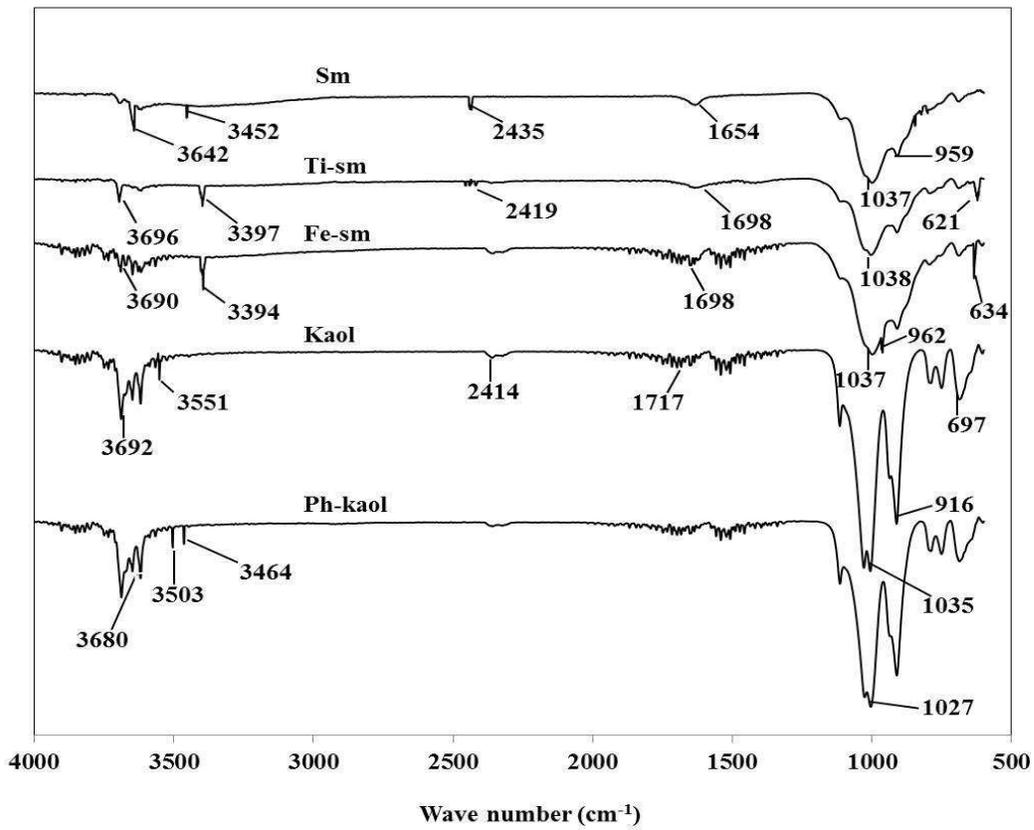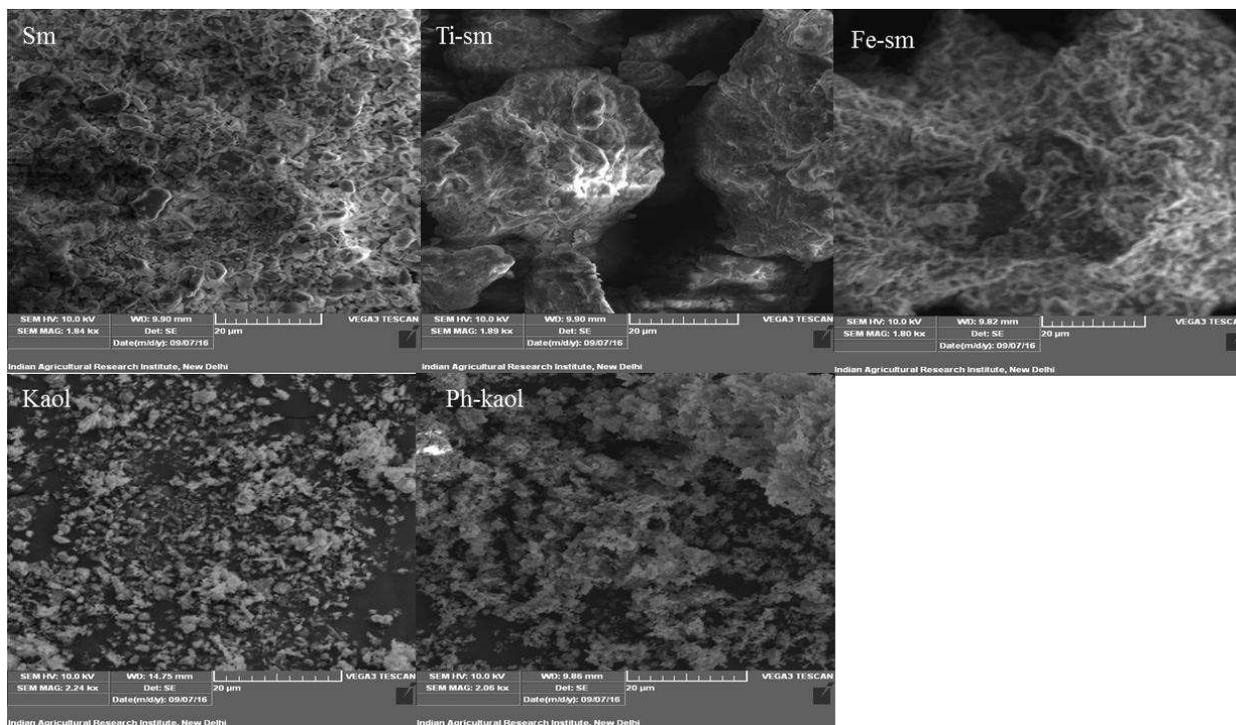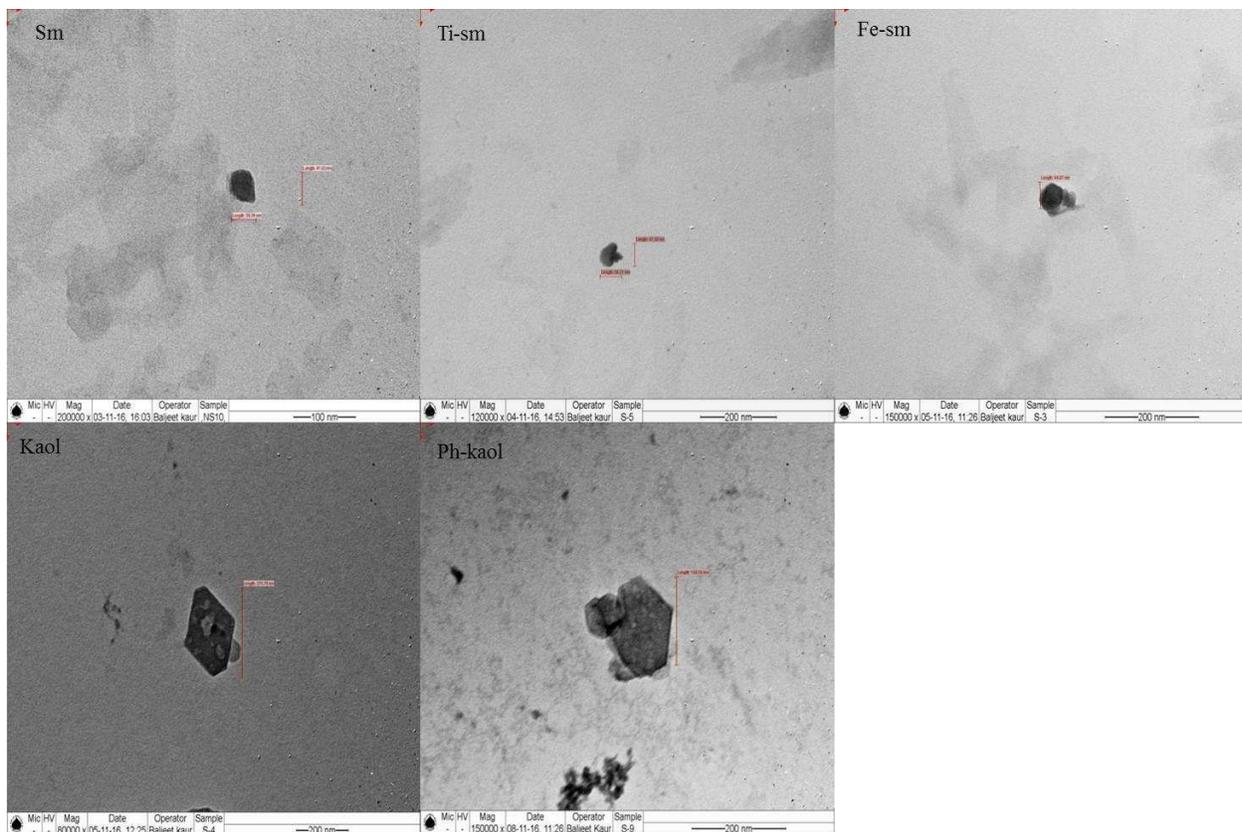
Fig. 2 FT-IR spectra of unmodified smectite (Sm), Ti-pillared smectite (Ti-sm), Fe-exchanged smectite (Fe-sm), unmodified kaolinite (Kaol) and phosphate-bound kaolinite (Ph-kaol)
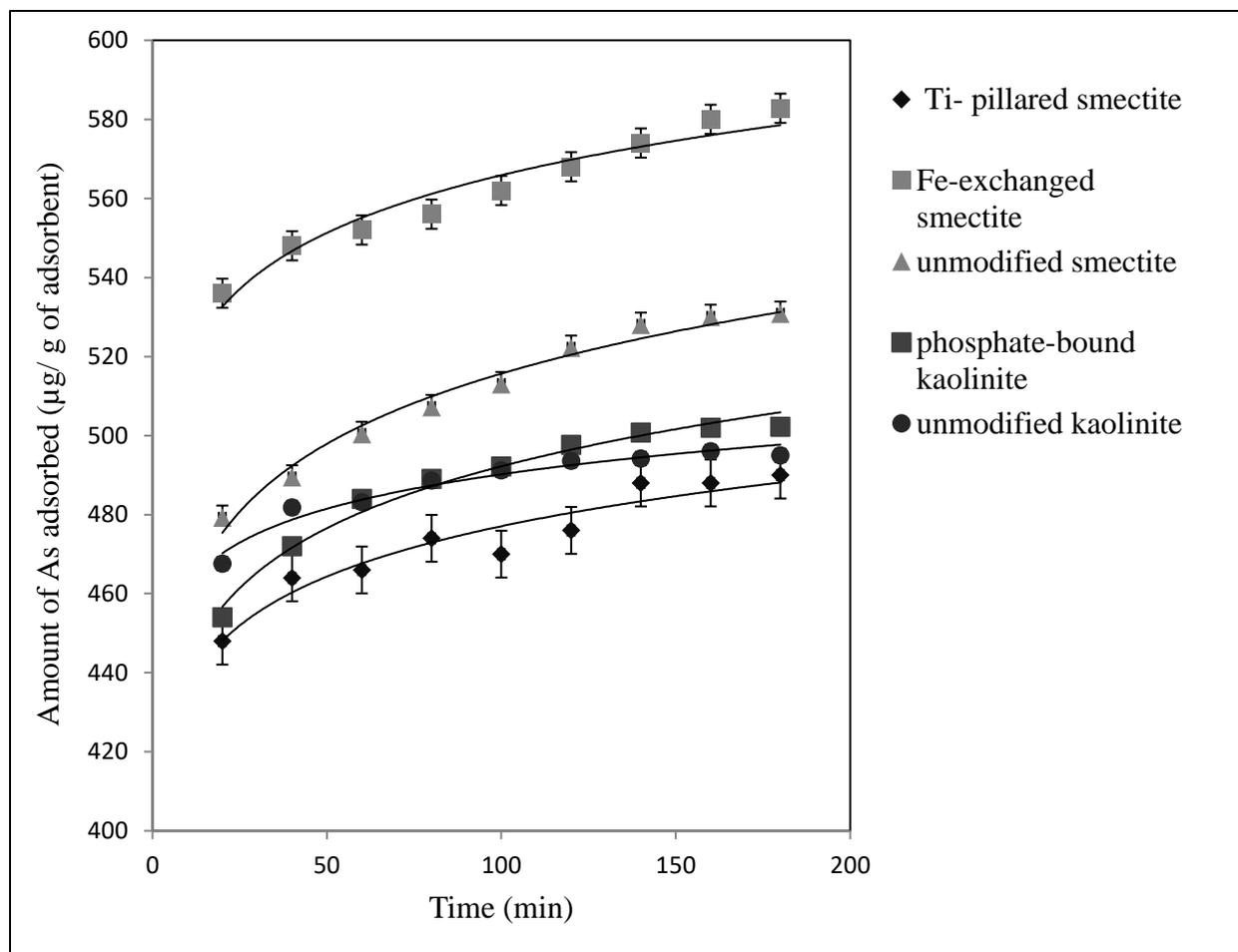
Fig. 3 SEM images of unmodified smectite (Sm), Ti-pillared smectite (Ti-sm), Fe-exchanged smectite (Fe-sm), unmodified kaolinite (Kaol) and phosphate-bound kaolinite (Ph-kaol)

Fig. 4 TEM images of unmodified smectite (Sm), Ti-pillared smectite (Ti-sm), Fe-exchanged smectite (Fe-sm), unmodified kaolinite (Kaol) and phosphate-bound kaolinite (Ph-kaol)

Fig. 5 Kinetics of arsenic adsorption onto unmodified, Ti-pillared, Fe-exchanged smectites, and unmodified and phosphate-bound kaolinites in aqueous system (the fitting curves represent the power function equation).
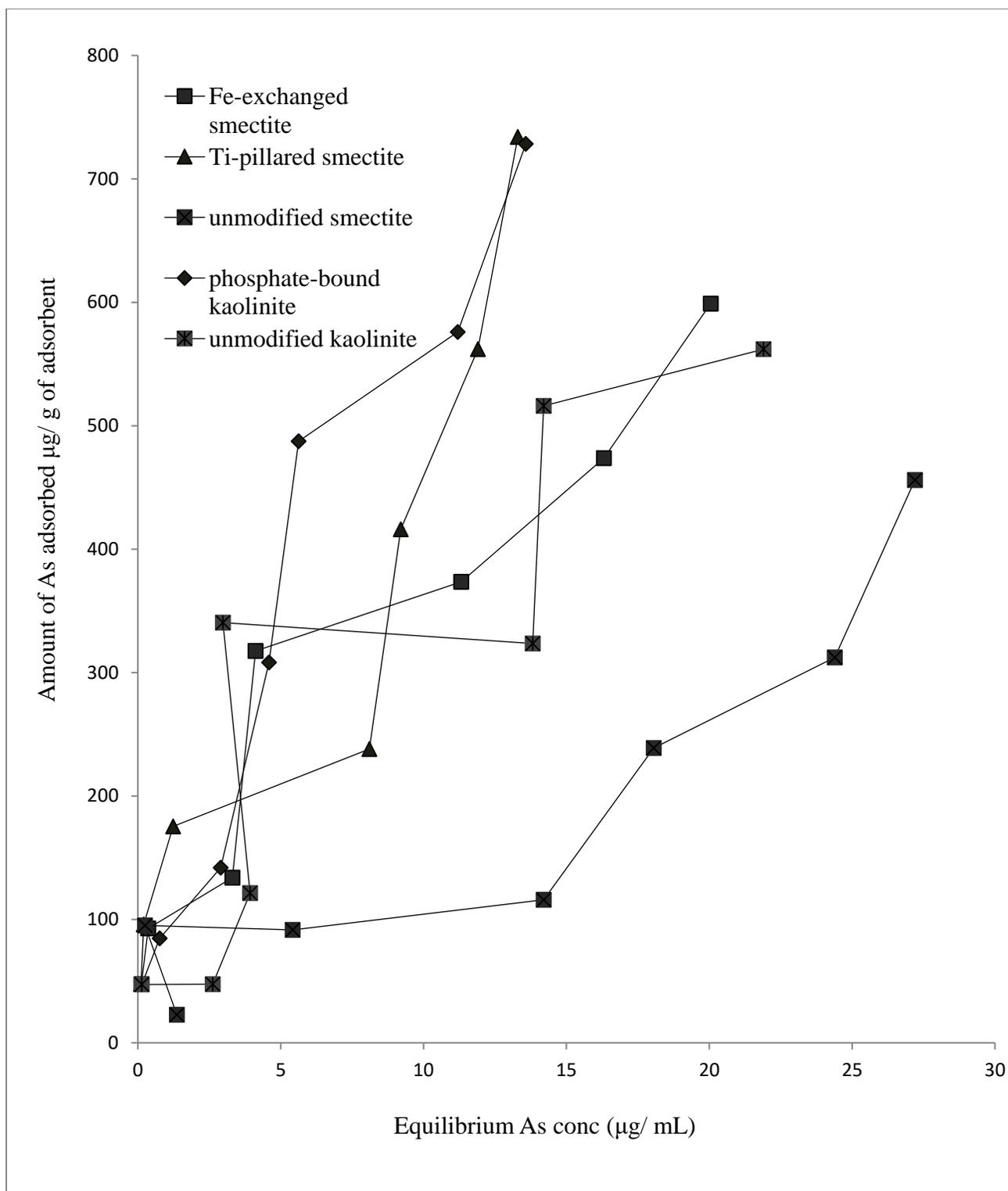
Fig. 6 Arsenic adsorption isotherm onto unmodified, Ti-pillared and Fe-exchanged smectites, and unmodified and phosphate-bound kaolinites in aqueous system (the curves were best fitted in Freundlich adsorption isotherm).
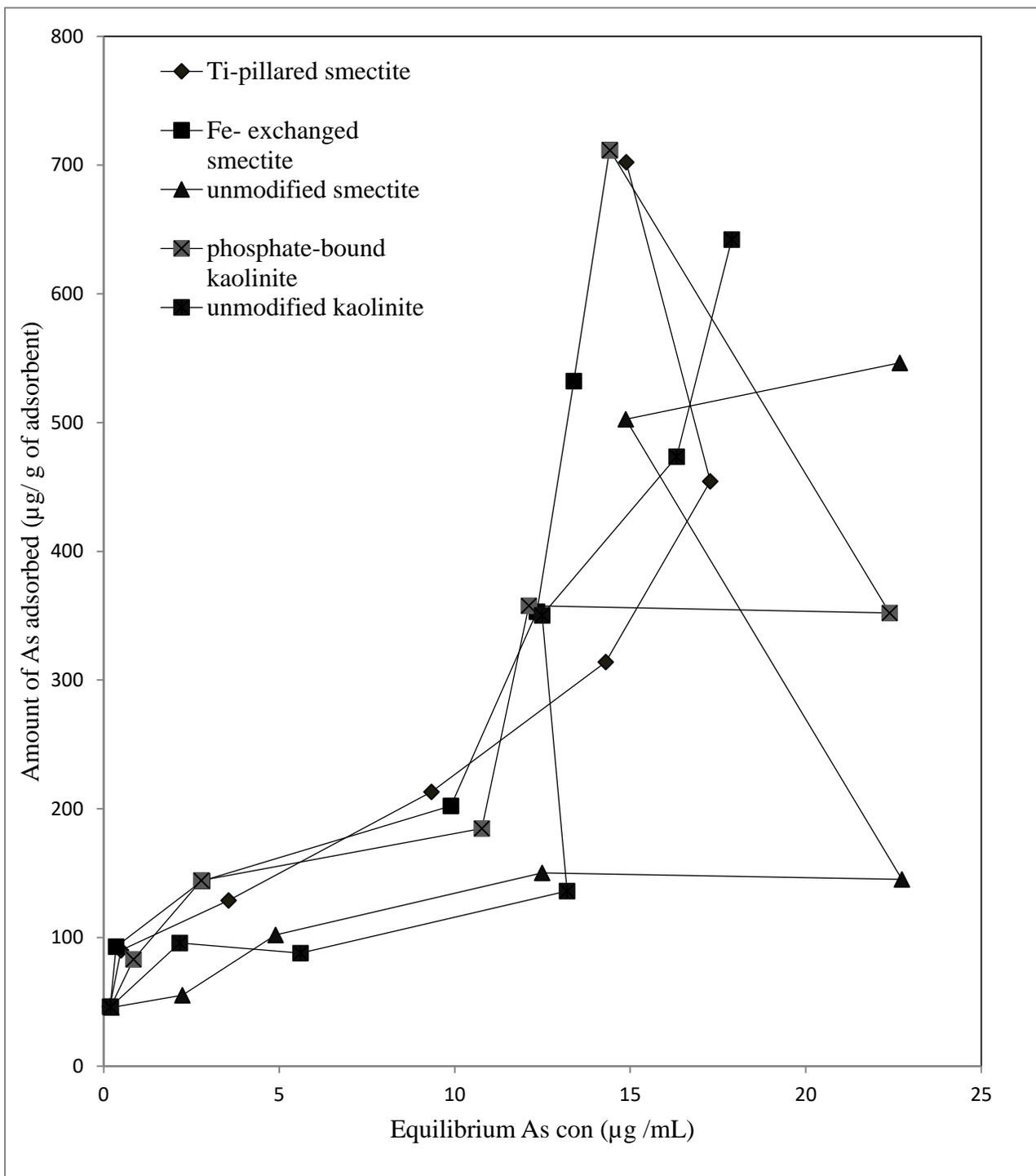
Fig. 7 Arsenic adsorption isotherm onto unmodified, Ti-pillared and Fe-exchanged smectites, and unmodified and phosphate-bound kaolinites in soil system (the curves were best fitted in Freundlich adsorption isotherm).